
NOVEL SEMICRYSTALLINE THERMOPLASTIC R-BAPB TYPE POLYIMIDE MATRIX REINFORCED BY GRAPHITE NANOPLAQUETS AND CARBON NANOPARTICLES

Vladimir E. Yudin¹, Joshua U.Otaigbe^{2*}, Lawrence T.Drzal³ and Valentin M. Svetlichnyi¹

¹Institute of Macromolecular Compounds, Russian Academy of Sciences,
199004 Saint Petersburg, V.O. Bolshoy pr., 31, Russia

²School of Polymers and High Performance Materials, University of Southern Mississippi,
118 College Drive #10076, Hattiesburg, MS 39406, USA

³Department of Chemical Engineering and Materials Science, Composite Materials and Structure Centre,
Michigan State University, East Lansing MI, 48824-1226, USA

(Received 9/06; accepted 10/06)

ABSTRACT

A new semicrystalline polyimide, based on 1,3-bis-(3,3',4,4'-dicarboxyphenoxy)benzene (R) and 4,4'-bis-(4-aminophenoxy)biphenyl (BAPB), was modified by exfoliated graphite nanoplatelets of different shape, sizes and structure. This R-BAPB type polyimide, with a molecular weight $M_w = 30000$ g/mol has a low melting temperature of 320°C and a melt zero shear viscosity of about 1000 Pa s at 340°C, making it possible to mix it with particulates using classical melt-blending technology. By using calorimetric and rheological measurements, this study reports a dramatic crystal nucleating effect of the polyimide caused by the special nanographite platelets. In addition, the study shows that classical melt blending of R-BAPB type PI with exfoliated graphite nanoplatelets can be used to prepare useful polyimide nanocomposites with the added benefit of possibly accelerating the crystallization process of the polyimide matrix. Further, it was observed that the time of crystallization at 300°C for the nanocomposites filled with 5 wt% nanographite platelets was about 10 ± 5 minutes, a value corresponding to one-half that of the unfilled R-BAPB type PI matrix.

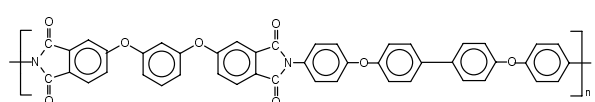
Keywords: Semicrystalline polyimide; crystallization; graphite nanoplatlet; nanocomposite; nucleation

1. INTRODUCTION

Polyimides (PIs) are considered to be one of the most important engineering plastics because of their excellent thermal stability, mechanical properties, and chemical resistance [1-3]. Although the PIs utilized for most applications are typically amorphous, the relative importance of crystallinity has led to some efforts to develop semicrystalline PIs that are thermoplastic [4-9]. These relatively new semicrystalline PIs exhibit processibility and thermomechanical properties that are comparable to that of typical poly(ether ether)ketone (PEEK) [10]. In addition, these semicrystalline PIs show attractive properties such as excellent oxidative stability, resistance to strong bases, and high adhesion properties, making them potentially widely applicable. A special characteristic of these new PI polymers is their ability to crystallize from the melt to form crystalline matrices for composite materials. It is noteworthy that prior semicrystalline PIs reported in the literature such as LARC-CPI [4], LARC CPI-2 [5], PI-2 [6], New TPI [7], TPEQ-ODPA [8] and

TPER-BPDA [9] have poor processability and very high melt viscosity at temperatures close to their thermal degradation when compared with the present polyimide system reported in this paper.

Recently [11, 12], we reported the crystallization behaviour of a new semicrystalline R-BAPB type PI:



Compared to the LARC-CPI, the advantages of the above R-BAPB type PI include low melting temperature $T_m \approx 320^\circ\text{C}$ ($T_g = 204^\circ\text{C}$) and a viscosity value of $\eta \approx 1000$ Pa s at 340°C (see Table 1). The relatively low melt processing temperatures (340 °C) of the R-BAPB type PI is significantly below its thermal degradation (~450 °C), as a result these polyimides are expected to find applications as thermoplastic semicrystalline matrices for fibre-reinforced composites and nanocomposites.

Table 1: Thermal and viscous properties of some high-performance thermoplastics.

Chemical Structure	Name	Tg °C	Tm °C	[η] Pa·s
	ULTEM-1000 GE	216	ND	$10^2\text{-}10^3$ (330-350°C)
	PEEK ICI	143	340	$10^3\text{-}10^4$ (340-360°C)
	LaRC-CPI NASA	220	360	$10^4\text{-}10^5$ (380°C)
	R-BAPB IMC RAS	205	320	$10^2\text{-}10^3$ (330-350°C)

Compared with the engineering thermoplastic PEEK, this R-BAPB type PI has a slow crystallization rate requiring at least 30 minutes at 280 ± 20 °C to crystallize completely.

Previous research has shown [11, 12] that in some cases, the addition of oligoimides with chemical structures similar to that of the main chain of R-BAPB lead to complete recrystallization of PIs after melting at 360°C. It was suggested that the main contribution of the oligoimides was through plasticization, allowing segmental chain mobility during crystallization, and not via nucleation. A similar effect is obtained by lowering the molecular weight of the PI; this, however, causes reduction in mechanical properties, rendering the polyimide inapplicable for composite materials. Crystallization was also enhanced [12, 13] by carbon fibres and nanoparticles, serving as nucleating agents resulting in transcrystallization.

In this paper, we report results of a study of several factors with potential influence on the crystallization of R-BAPB type PI. The study examined the nucleating effects of three carbon based nanoplatelets namely, graphite nanoplatelets and carbon cones, which are added in very low concentrations to the R-BAPB type PI matrix. The results of this study complement a number of prior investigations reported

in the literature that deal with polymer crystallization by carbon nanoparticles [14-20]. Further, the study may stimulate a better understanding of the rational synthesis and processing of polyimides with prescribed morphology and properties for a number of potential useful applications.

2. EXPERIMENTAL

2.1 Carbon and Nanographite Particles

Graphite nanoplatelets ~300 nm in size and only ~10 nm in thickness were produced by heating to above ~280°C. The starting material was an intercalated graphite containing a mixture of sulphuric and nitric acid remains in its galleries (GRAFOIL™) obtained from GRAFTECH Inc., USA. Heating causes the acid intercalated graphite to exfoliate and expand by several hundred percent.

The Carbon Cones (CONE™) were supplied by n-TEC Co., Norway. These CONE™ particles consist of 20 wt% carbon cones, 70 wt% carbon discs, and 10 wt% carbon black (impurities). The carbon cones have a length of 0.3 – 0.8 mm, maximum base diameter of 1-2 mm and wall thickness of 20 – 50 nm. The discs have a diameter of 0.8 – 3 mm and thickness of 20 – 50 nm.

2.2 Preparation of polyimides (PIs)

Poly(amic acid) (PAA) was obtained by polycondensation of 1,3-bis(3,3',4,4'-dicarboxyphenoxy)benzene (R) and 4,4'-bis-(4-aminophenoxy)biphenyl (BAPB) supplied by Wakayama Seika Co., Ltd. (Japan) in a 25% solution of N-methyl-2-pyrrolidone (NMP) at 25°C. The polymer chains were fully endcapped with phthalic anhydride (PA) to control the molecular weight and maximize the PI thermal stability [21]. The specific R-BAPB type PAA used in this study had an average molecular weight $\langle M_w \rangle \sim 30000$ g/mole. The R-BAPB type PAA was converted to the respective R-BAPB type PI powder by using solution imidization techniques reported in the literature [22, 23].

2.3 Preparation of Nanocomposites

A HAAKE MiniLab® Micro Compounder was used for melt mixing of the R-BAPB type PI with the exfoliated graphite nanoplatelets and CONE™ particles. Five grams mixtures of R-BAPB type PI and exfoliated graphite nanoplatelets and CONE™ particles were extruded using a Micro Compounder to obtain nanocomposites with concentrations of 5 wt% exfoliated graphite nanoplatelets or CONE™ particles in the polyimide. Using material densities of 1.30 g/cm³ for PI and ~ 2 g/cm³ for carbon nanoparticles, the corresponding volume concentrations of carbon nanoparticles in the nanocomposite was found to be ~ 3 vol%. The melt compounding was carried out at a temperature of 350°C for ten minutes using a screw speed of 100 rpm. A MicroInjector (DACA Instruments Company) was used to prepare the nanocomposite samples with dimensions of length = 20 mm, width = 5 mm, and thickness = 1 mm. The barrel temperature was maintained at 380°C and the mold temperature was 90°C. These samples were used for dynamic mechanical measurements as described in the next section.

2.4 Measurements

A strain-controlled dynamic rheometer ARES® from TA Instruments was used to measure the dynamic and steady shear viscosity of the polymers and nanocomposites in the cone and plate configuration following standard procedures. The diameter of the plate was 25 mm and the cone angle was 0.1 rad. Nitrogen was used as the heating gas for temperature control. To perform the melt viscosity measurements, we used disks that were compression molded at 350°C from blends of the R-BAPB type PI with the graphite nanoplatelets or CONE™ particles. (Note that the

blends of the polymer and nanoparticles just mentioned were obtained with the aid of HAAKE MiniLab® Micro Compounder as already described in Section 2.3). The disk was subsequently placed between the plates of the rheometer that were preheated to the desired temperature of 360°C at which the sample was melted completely in 10 min. Thereafter, the sample was cooled to 300°C at a rate of ~20 K/min and allowed to equilibrate at this temperature for 1 min prior to recording of the data. Dynamic time sweeps were performed using the small amplitude oscillation shear mode at a frequency of 1 rad/s and a linear strain of 1 %.

The torsion rectangular fixture of the ARES was used for testing the solid nanocomposites prepared with the aid of MicroInjector (DACA Instruments Company) as already described in Section 2.3. The samples were held in tension between the upper and lower tool. Dynamic Temperature Ramp Tests were performed using the oscillation mode at a frequency of 1 rad/s and a strain of 0.1 %. The temperature ramp rate used was 5°C/min.

Wide angle X-ray diffraction (WAXD) was measured by a MiroMax007 diffractometer (Rigaku Denki Co. Ltd.) operating at 40 kV and 20 mA. The samples were exposed to CuK α X-ray beams monochromatized with a graphite monochromator through a pinhole collimator of 0.3 mm in diameter.

Thermogravimetric Analysis (TGA), and Differential Scanning Calorimetry (DSC) curves were recorded with a comprehensive Perkin-Elmer thermal Analysis 7 system. The TGA measurements were conducted using 5 to 10 mg samples contained in a platinum crucible with a heating rate of 10°C under a nitrogen atmosphere. DSC was performed on 3-6 mg samples contained in a platinum crucible with a heating rate of 10°C/min under a nitrogen atmosphere.

3. RESULTS AND DISCUSSION

Fig. 1 shows SEM photomicrographs of the PI nanocomposite filled with 3 wt% exfoliated graphite nanoplatelets. Clearly, this Figure shows evidence of a relatively good dispersion of the graphite nanoplatelets in the polymer matrix. Melt rheology measurements at 360°C show that 5 wt % loading of the exfoliated graphite nanoplatelets in the thermoplastic R-BAPB type PI significantly increased the viscosity of the material especially at low frequencies or at low shear rates (Fig. 2). The viscosity increase and the associated shear thinning

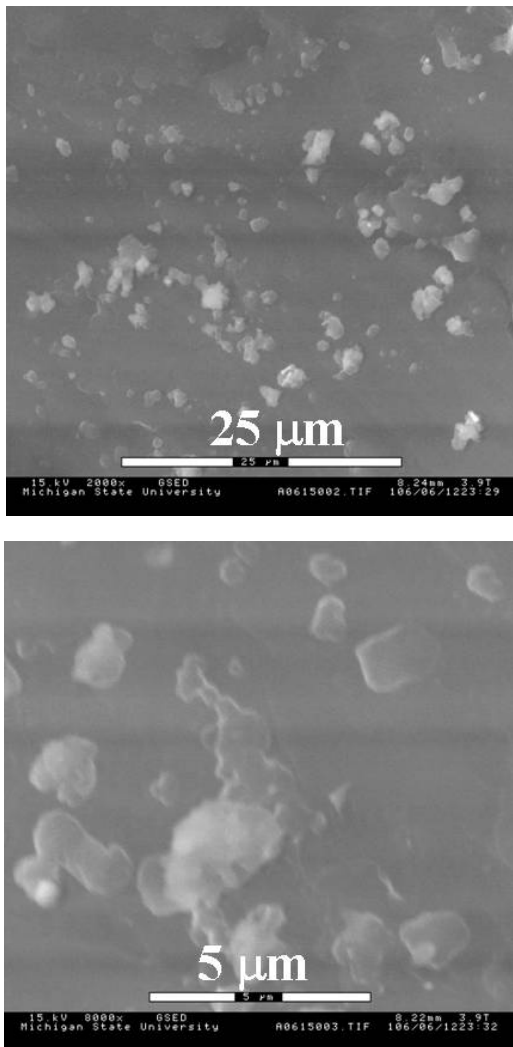


Fig. 1: SEM photomicrograph of the fracture surface of R-BAPB type PI nanocomposites filled with 3 wt% of exfoliated graphite nanoplatelets.

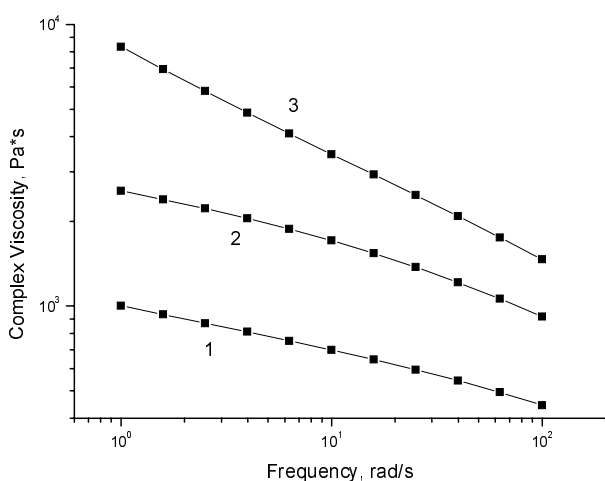


Fig. 2: Frequency dependence of Complex Viscosity for R-BAPB type PI (1) and nanocomposites based on R-BAPB and 5 wt% of CONE™ particles (2) or 5 wt% exfoliated graphite nanoplatelets (3). $T = 360^\circ\text{C}$, $\varepsilon = 1\%$.

(viscosity decrease with frequency) exhibited by the nanocomposites was found to be more significant in the case of the PI nanocomposite filled with the exfoliated graphite nanoplatelets than that filled with CONE™ particles. This observation is thought to be due to the relative high aspect ratio ($\sim 10^4$) of the exfoliated graphite nanoplatelets compared to that of the CONE™ discs (~ 30). The strong shear thinning behaviour of the PI filled with the exfoliated graphite nanoplatelets appear to be indicative of the formation of a shear-sensitive structure that is akin to a fractal gel. The results suggest that useful, melt-processible PI nanocomposites can be prepared by classical melt blending methods at a filler loading not to exceed 5 wt %. Higher concentrations of the exfoliated graphite nanoplatelets result in a melt with intractable viscosity for conventional melt blending. If a higher loading of the exfoliated graphite nanoplatelets in the PI is desired, decreasing the aspect ratio by milling of the exfoliated graphite nanoplatelets may alleviate the viscosity problem just mentioned. This hypothesis will be tested in a future proposed research.

In this study, we used rheology measurements similar to the ones reported by Grizzuti and coworkers [24,25] to monitor the crystallization process of R-BAPB type PI filled with 0 and 5 wt.% exfoliated graphite nanoplatelets or CONE™ particles (Fig. 3). The rheological signature of the crystallization process at 300°C depicted in Fig. 3 shows that the viscosity of the PI filled with the exfoliated graphite nanoplatelets increases more rapidly than that of the pure PI or PI filled with the CONE™ particles. Note that the data of Fig. 3 was collected after the samples were initially

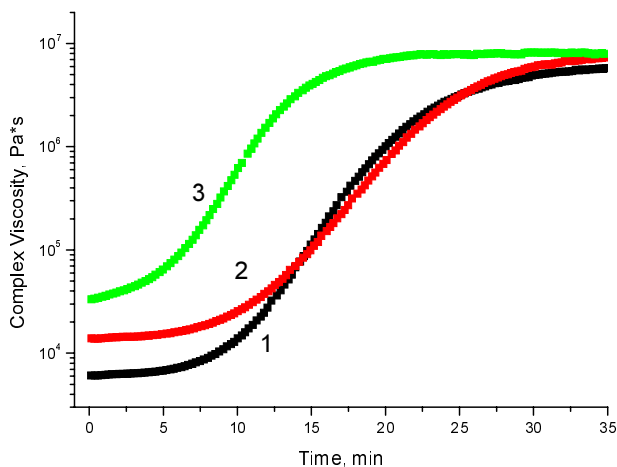


Fig. 3: Time Dependence of Complex viscosity at temperature $T = 300^\circ\text{C}$ for R-BAPB type PI (1) and nanocomposites based on R-BAPB and 5 wt% CONE™ particles (2) or 5 wt% exfoliated graphite nanoplatelets (3). Test type is Dynamic Time Sweep, $\omega = 1 \text{ rad/s}$ and $\varepsilon = 1\%$

melted at 360°C for 10 min in the rheometer. The strong viscosity increase is ascribed to crystallization of the samples as confirmed by the DSC results. The DSC scans of the samples after complete crystallization confirmed their crystallinity with the melting point $T_m = 320^\circ\text{C}$ and heat of fusion $\Delta H = 27 \pm 2 \text{ J/g}$. The heat of fusion for a 100% crystalline PI sample was estimated using a combination of DSC and WAXD techniques as previously reported [12]. A linear regression fit of the data resulted in an extrapolated heat of fusion value $\Delta H = 90 \text{ J/g}$ for the 100% crystalline R-BAPB type PI sample. The maximum value of crystallinity which was obtained in our experiments did not exceed an average of 30% for both R-BAPB type PI matrix and their nanocomposites. From the preceding results, it can be concluded that incorporation of exfoliated graphite nanoplatelets in R-BAPB type PI can nucleate the crystallization process of the PI matrix at 300°C thereby decreasing the crystallization time (Fig. 4) without changing the overall percent crystalline content of the pure R-BAPB matrix (i.e., ~30% crystallinity).

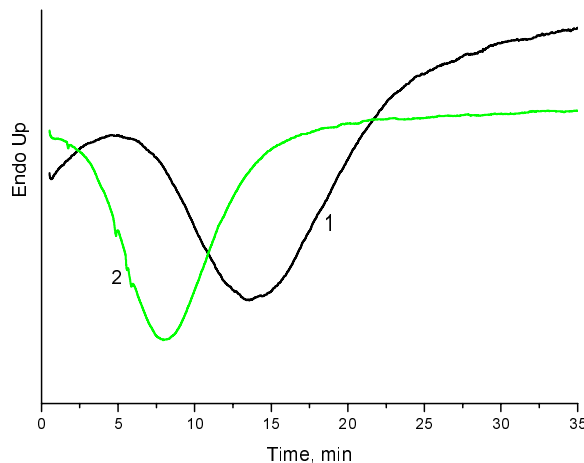


Fig. 4: The DSC thermograms showing heat flow as a function of heating time of pure R-BAPB type PI (1) and nanocomposite based on R-BAPB and 5 wt% exfoliated graphite nanoplatelets (2), which were isothermally crystallized at 300°C.

The specific role of the large basal graphene surface in the exfoliated graphite nanoplatelets on the crystallization of the PI of this study was investigated by comparing the nucleating effect of the exfoliated graphite nanoplatelets with the CONE™ particles used. Comparative WAXD analyses of pure (i.e., without PI matrix) exfoliated graphite nanoplatelets and CONE™ particles are presented in Fig. 5. A very

sharp peak at ~26.5 degrees in this Figure is characteristic of the graphitic layered structure of exfoliated graphite nanoplatelets while the broad amorphous halo is typical of the CONE particles. Fig. 5 supports the conclusion suggested earlier in [20] for crystallization of polycarbonate modified by vapour grown carbon nanofibres, that the nucleating effect can be caused by interaction between the graphite and the phenyl groups of the PI.

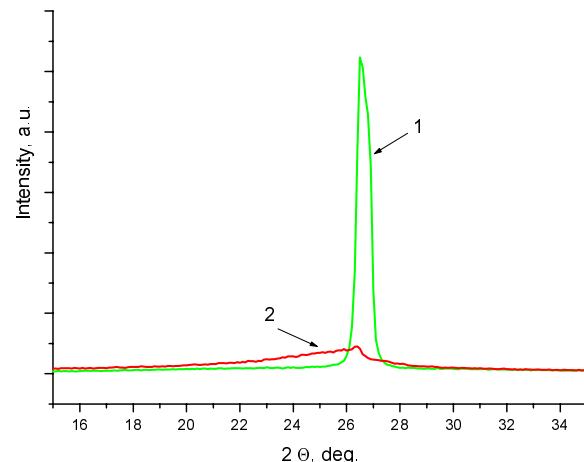


Fig. 5: Wide angle X-ray diffraction scans for exfoliated graphite nanoplatelets (1) and CONE™ particles (2).

Fig. 6 shows dynamic mechanical data for R-BAPB type nanocomposite based on 3 wt% exfoliated graphite nanoplatelets and for unfilled Ultem®-1000. These data were obtained by using dynamic temperature ramp test program of the ARES rheometer as already described. It can be seen from

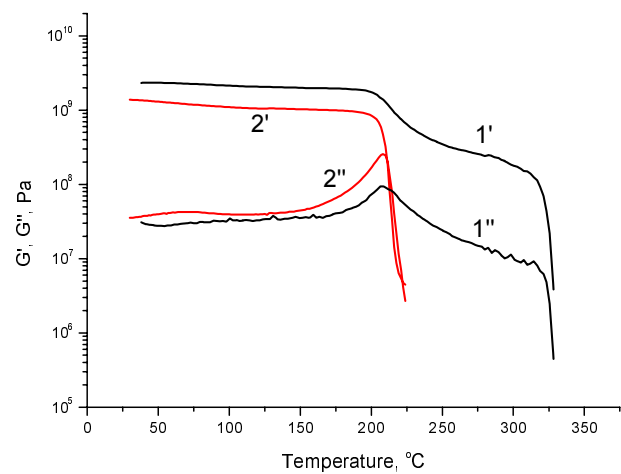


Fig. 6: Temperature dependencies of shear storage G' and loss G'' moduli for nanocomposite based on R-BAPB type PI matrix and 3 wt% exfoliated graphite nanoplatelets (1', 1'') and for ULTEM®-1000 (2', 2'')

this Figure that in the nanocomposite based on semicrystalline R-BAPB type PI matrix (percent crystallinity $\sim 30\%$) the storage modulus G' (Fig. 6, curve 1') maintains a high value of ~ 0.5 GPa up to the melting temperature of about 300°C . For the commercial Ultem-1000 the modulus G' (Fig. 6, curve 2') drops abruptly at the glass transition temperature of 200°C . The data of Fig. 5 indicate that enhanced PI matrix crystallization caused by the exfoliated graphite nanoplatelets can significantly increase the thermal stability by almost 100°C of the PI nanocomposite even at very small filler concentrations (3 wt.%) and small strain amplitudes (0.1%) compared with that based on completely amorphous PI such as Ultem[®]-1000.

TGA scans (Fig. 7) show approximately the same initiation of thermal decomposition for R-BAPB PI/exfoliated graphite nanoplatelets nanocomposite as for Ultem[®]-1000, but the coke residue of the former is about ten percent higher than that of the Ultem[®]-1000.

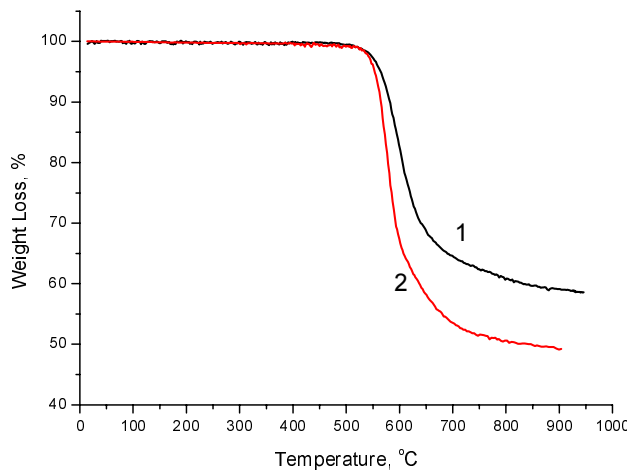


Fig. 7: TGA scans of nanocomposite based on R-BAPB type PI and 3 wt% exfoliated graphite nanoplatelets (1) and Ultem[®]-1000 (2). Nitrogen atmosphere.

4. CONCLUSIONS

This study shows that a new semicrystalline polyimide matrix R-BAPB has a relatively low melting temperature (320°C) and low viscosity at 360°C and is melt processible using traditional polymer processing methods such as extrusion and injection molding. Melt blending of R-BAPB type PI with small amounts of exfoliated graphite nanoplatelets yields useful nanocomposites in which the crystallization of the PI matrix from the melt is significantly accelerated by the presence of the basal surfaces of the graphite nanoplatelets. The strongest nucleating effect is observed for fillers with large areas of graphitic basal

plane such as that in exfoliated graphite nanoplatelets, for which the maximum degree of crystallinity of the polyimide matrix can be recovered. The time of crystallization for the nanocomposites filled with 5 wt% exfoliated graphite nanoplatelets decreased to about 10 ± 5 minutes at 300°C , approximately one-half the time needed for crystallization of the unfilled R-BAPB type PI. The rheological behaviour, crystallization ability and mechanical properties of the semicrystalline R-BAPB matrix can be modified and controlled by blending with small concentrations of graphite nanoplatelets, making it useful as a potential matrix for other advanced composites for high temperature applications. Based on these preliminary observations an intensive study currently underway is aimed at exploring use of different graphite nanoplatelets of different sizes (aspect ratio) and surface modifications in various semicrystalline thermoplastic polyimides with a goal of obtaining optimal nanofiller dispersions.

ACKNOWLEDGEMENTS

Financial support of this work by the U.S. National Science Foundation under contract grant numbers DMR-0213883 and CTS-0317646, and by the Russian Fund of Basic Research under contract grant number 04-03-32470-a is gratefully acknowledged.

References:

1. Bessonov, M.I., Koton, M.M., Kudryavtsev, V.V. and Laius, L.A., "Polyimides-Thermally Stable Polymers", Plenum, New York (1987).
2. Wilson, D., Stenzenberger, H.D. and Hergenrother, P.M. (Eds.), "Polyimides", Chapman and Hall, New York (1990).
3. Ghosh, M.K. and Mittal, K.L. (Eds.). "Polyimides: Fundamentals and Applications", Marcel Dekker, New York (1996).
4. Hergenrother P.M. and Havens, S.J., "Adhesive properties of LARC-CPI, a new semi-crystalline polyimide", SAMPE J., **24** (1988), 13-18.
5. Brandom, D.K. and Wilkes, G.L., "Study of the multiple melting behavior of the aromatic polyimide LaRC CPI-2", Polymer, **35** (1994), 5672-5677.
6. Cheng, S.Z.D., Mittleman, M.L. Janimak, J.J., Shen, D., Chalmers, T.M., Lien, H.-S., Tso, C.C., Gabori, P.A. and Harris, F.W., "Crystal-structure, crystallization kinetics and morphology of a new polyimide", Polym. Int., **29** (1992), 201-208.
7. Srinivas, S., Caputo, F.E., Graham, M., Gardner, S., Davis, R.M., McGrath, J.E. and Wilkes, G.L., "Semicrystalline Polyimides Based on Controlled Molecular Weight Phthalimide End-Capped 1,3-Bis(4-aminophenoxy)benzene and 3,3',4,4'-Biphenyltetracarboxylic Dianhydride: Synthesis, Crystallization, Melting, and Thermal Stability",

- Macromolecules*, **30** (1997), 1012-1022.
8. **Srinivas, S., Graham, M., Brink, M.H., Gardner, S., Davis, R.M., McGrath, J.E. and Wilkes, G.L.**, “Influence of melt stability on the crystallization of bis(4-aminophenoxy)benzene-oxydiphthalic anhydride based polyimides”, *Polym. Eng. Sci.*, **36** (1996), 1928-1940.
 9. **Ratta, V., Ayambem, A., Young, R., McGrath, J.E. and Wilkes, G.L.**, “Thermal stability, crystallization kinetics and morphology of a new semicrystalline polyimide based on 1,3-bis(4-aminophenoxy) benzene and 3,3', 4,4"-biphenyltetracarboxylic dianhydride”, *Polymer*, **41** (2000), 8121-8138.
 10. **Gao, S.L. and Kim, J.K.** “Semicrystalline polyimide matrices for composites: Crystallization and properties”, *J. Appl. Polym. Sci.*, **83** (2002), 2873-2882.
 11. **Yudin, V.E., Svetlichnyi, V.M., Gubanova, G.N., Didenko, A.L., Sukhanova, T.E., Kudryavtsev, V.V., Ratner, S. and Marom, G.**, “Correlation among crystalline morphology of PEEK, interface bond strength, and in-plane mechanical properties of carbon/PEEK composites”, *J. Appl. Polym. Sci.*, **84** (2002), 1155-1167.
 12. **Yudin, V.E., Svetlichnyi, V.M., Gubanova, G.N., Didenko, A.L., Popova, E.N., Sukhanova, T.E., Grogoriev, A.I. and Kostereva, T.A.**, “Influence of crystallinity of R-BAPB type polyimide matrix on thermal and mechanical properties of carbon fibre reinforced composites”. In the book “Polyimides and other high temperature polymers” (Ed. K.L.Mittal), **3** (2005), 229.
 13. **Yudin, V.E., Svetlichnyi, V.M., Shumakov, A.N., Letenko, D.G., Feldman, A.Y. and Marom, G.**, “The Nucleating Effect of Carbon Nanotubes on Crystallinity in R-BAPB-Type Thermoplastic Polyimide”, *Macromol. Rapid Commun.*; **26** (2005), 885-888.
 14. **Assouline, E., Lustiger, A., Barber, A., Cooper, C.A., Klein, E., Wachtel, E. and Wagner, H.D.**, “Nucleation ability of multiwall carbon nanotubes in polypropylene composites”, *J. Polym. Sci.: Part B: Polym. Phys.* **41** (2003), 520-527.
 15. **Lai, M., Li, J., Yang, J., Liu, J., Tong, X. and Cheng, H.**, “The morphology and thermal properties of multi-walled carbon nanotube and poly(hydroxybutyrate-co-hydroxyvalerate) composite”, *Polym. Int.*; **53** (2004), 1479-1484.
 16. **Bhattacharyya, A.R., Sreekumar, T.V., Liu, T., Kumar, S., Ericson, L.M., Hauge R.H. and Smalley, R.E.**, Crystallization and orientation studies in polypropylene/single wall carbon nanotube composite”, *Polymer*; **44** (2003), 2373-2377.
 17. **Sandler, J., Broza, G., Notle, M., Schulte, K., Lam, Y.M. and Shaffer, M.S.P.**, “Crystallization of carbon nanotube and nanofiber polypropylene composites”, *J. Macromol. Sci-Phys.*, **B42** (2003), 479-488.
 18. **Ryan, K.P., Lipson, S.M., Drury, A., Cadek, M., Ruether, M., O'Flaherty, S.M., Barron, V., McCarthy, B., Byrne, H.J., Blau, W.J. and Coleman, J.N.**,
- “Carbon-nanotube nucleated crystallinity in a conjugated polymer based composite”, *Chem. Phys. Lett.* **391** (2004), 329-333.
19. **Coleman, J.N., Cadek, M., Blake, R., Nicolosi, V., Ryan, K.P., Belton, C., Fonseca, A., Nagy, J.B., Gun'ko, Y.K. and Blau, W.J.**, “High performance nanotube-reinforced plastics: Understanding the mechanism of strength increase”, *Adv. Funct. Mater.* **14** (2004), 791-798.
 20. **Takahashi, T., Yonetake, K., Koyama, K., Kikuchi, T.**, “Polycarbonate Crystallization by Vapor-Grown Carbon Fiber with and without Magnetic Field”, *Macromol. Rapid Commun.* **24** (2003), 763-767.
 21. **Srinivas, S., Graham, M., Brink, M.H., Gardner, S., Davis, R.M., McGrath, J.E. and Wilkes, G.L.**, *Polym. Eng. Sci.*, **36** (1996), 1928-1940.
 22. **Nesterov, V.V., Kudryavtsev, V.V., Svetlichnyi, V.M., Gazdina, N.V., Belnikevich, N.G., Kurenbin, O.I. and Zhukova T.I.**, “Study of soluble polyamic acids and polyester imides by methods of exclusion liquid chromatography”, *Polymer Science, Ser.A*, **39** (1997), 1387-1391.
 23. **Polotskaya, G.A., Kuzhnetsov, Y.P., Anikin, A.V., Lukashova, N.V., Zhukova, T.I., Svetlichnyi, V.M., Kudryavtsev, V.V., Eremina, M.A.**, “Chemical-structure and gas-separating properties of aromatic polyesterimides membranes”, *Polymer Science, Ser.A*, **34** (1992), 107-112.
 24. **Coppola, S., Balzano, L., Giuffredi E., Maffettone, P.L and Grizzuti, N.**, “Effects of the degree of undercooling on flow induced crystallization in polymer melts”, *Polymer*, **45** (2004), 3249-3256.
 25. **Acierno, S., Palomba, B., Winter, H.H. and N.Grizzuti**, “Effect of molecular weight on the flow-induced crystallization of isotactic poly(1-butene)”, *Rheol Acta*, **42** (2003), 243-250.